nature neuroscience

Bistability of cerebellar Purkinje cells modulated by sensory stimulation

Yonatan Loewenstein[1–3,6], Séverine Mahon[4,6], Paul Chadderton[4], Kazuo Kitamura[4], Haim Sompolinsky[2,5], Yosef Yarom[1,2] & Michael Häusser[4]

A persistent change in neuronal activity after brief stimuli is a common feature of many neuronal microcircuits. This persistent activity can be sustained by ongoing reverberant network activity or by the intrinsic biophysical properties of individual cells. Here we demonstrate that rat and guinea pig cerebellar Purkinje cells *in vivo* show bistability of membrane potential and spike output on the time scale of seconds. The transition between membrane potential states can be bidirectionally triggered by the same brief current pulses. We also show that sensory activation of the climbing fiber input can switch Purkinje cells between the two states. The intrinsic nature of Purkinje cell bistability and its control by sensory input can be explained by a simple biophysical model. Purkinje cell bistability may have a key role in the short-term processing and storage of sensory information in the cerebellar cortex.

Persistent firing of neurons after a transient stimulus is a common feature of sensory processing in neural circuits that has been shown to be associated with short-term memory tasks[1]. Hebb proposed that such persistent firing states are generated by cell assemblies with mutually reinforcing excitatory feedback connections. Indeed, recent theoretical and experimental work[2–4] has shown that local recurrent networks are capable of generating such sustained firing patterns. An alternative possibility is that persistent firing is sustained by the intrinsic properties of the neuron[5]. Several neuronal types show bistable behavior: brief excitation produces a prolonged increase in firing rate through activation of persistent inward currents that maintain depolarization[5–8]. Some neurons show multiple persistent firing states that reflect the history of their synaptic inputs[9]. Theoretically, single cell bistable or multistable states can function as short-term memory buffers or enhance the short-term memory capabilities of excitatory recurrent networks[4,5,10–12].

In contrast to the cerebral cortex, the cerebellum lacks a prominent recurrent excitatory synaptic network. Purkinje cells provide the sole output of the cerebellar cortex. They receive excitatory input from two distinct sources, the parallel fibers and the climbing fibers, and exert inhibitory control on their targets in the deep cerebellar nuclei. Each Purkinje cell is innervated by over 10^5 parallel fibers, which synapse on its elaborate leaf-like dendritic tree. Each Purkinje cell also receives input from a single climbing fiber axon, originating from a neuron in the inferior olive. The climbing fiber wraps around the proximal dendrites of the Purkinje cell, making hundreds of synaptic contacts. Purkinje cells can fire spontaneous sodium action potentials (known as 'simple spikes') in the absence of synaptic excitation[13]. In response to climbing fiber activation, they generate a stereotypic discharge pattern called a complex spike, which can be distinguished from ongoing simple spikes both intracellularly and extracellularly[14].

Previous intracellular *in vitro* studies have shown that Purkinje cells can show both spontaneous and current-evoked bistable behavior that is correlated with intermittent periods of simple spike discharge[6,15]. However, bistability in Purkinje cells *in vivo* and its potential implications for cerebellar information processing have not yet been investigated. Here we show that Purkinje cells *in vivo* show prominent ongoing bistability of membrane potential and spike output. Notably, the state of the neuron can be controlled by sensory-evoked climbing fiber input that can induce state transitions in both directions, triggering prolonged increases or decreases in the simple spike firing rate.

RESULTS

Purkinje cell membrane potential is bistable *in vivo*

To explore the dynamic interplay between intrinsic properties and physiological synaptic inputs in Purkinje cells, we obtained *in vivo* whole-cell recordings from rat and guinea pig Purkinje cells located in the cerebellar vermis and hemispheres. Purkinje cells, identified from the spontaneous occurrence of complex spikes at their characteristic frequency (~1 Hz)[14], showed transitions in membrane potential between a hyperpolarized state ('down state') and a depolarized state ('up state'). The hyperpolarized state was quiescent (that is, devoid of any simple spike activity), whereas the depolarized state was usually associated with simple spike discharge (**Fig. 1a**,**b**, left). Transitions between the down state and the up state were observed at either perisomatic (**Fig. 1a**) or dendritic (**Fig. 1b**) locations, and the existence of these two distinct states was apparent in the bimodal distribution of the membrane

[1]Department of Neurobiology, [2]The Interdisciplinary Center for Neural Computation, and [5]Racah Institute of Physics, The Hebrew University of Jerusalem, Jerusalem 91904, Israel. [3]Department of Brain and Cognitive Sciences, The Massachusetts Institute of Technology, Cambridge, Massachusetts 02139, USA. [4]Wolfson Institute for Biomedical Research and Department of Physiology, University College London, Gower Street, London WC1E 6BT, UK. [6]These authors contributed equally to this work. Correspondence should be addressed to Y.L. (yonatanl@mit.edu) or S.M. (s.mahon@ucl.ac.uk).

Published online 23 January 2005; doi:10.1038/nn1393

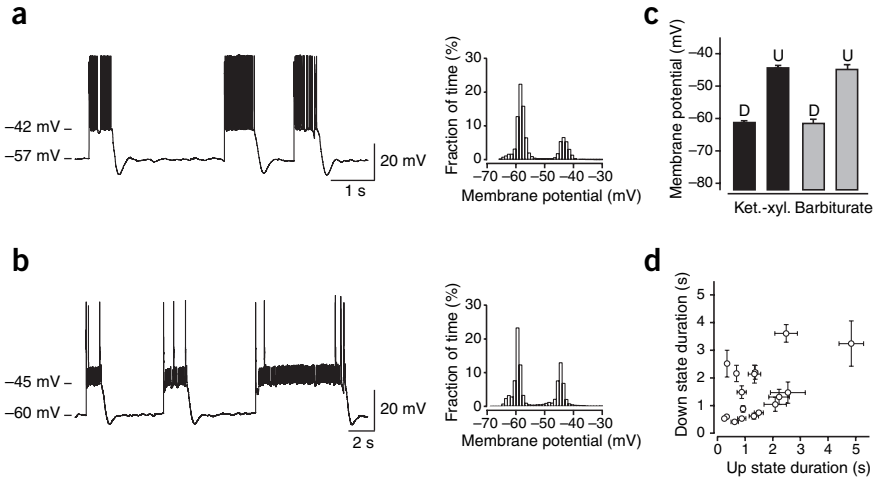

Figure 1 Spontaneous membrane potential bistability in Purkinje cells *in vivo*. (**a**) Left: whole-cell perisomatic recording of a rat Purkinje cell showing membrane potential fluctuations between two distinct states: a hyperpolarized quiescent state ('down state') and a depolarized spiking state ('up state'). Right: the corresponding histogram of the membrane potential calculated from 84 s of recording (bin size 1 mV). (**b**) Presumed distal dendritic whole-cell recording of a rat Purkinje cell showing similar up and down state transitions (left) as reflected in the bimodal distribution of the membrane potential (right, 100 s of recording, bin size 1 mV). (**c**) Comparison of the average values of the two membrane potential states (down state, D; up state, U) obtained under different anesthetics (ketamine-xylazine (Ket.-xyl.), $n = 24$ Purkinje cells; barbiturate, $n = 5$ Purkinje cells). (**d**) Relationship between the duration of down and up states. Each point corresponds to a single Purkinje cell. Error bars represent s.e.m.

potential (**Fig. 1a**,**b**, right). A dip test[16], which gives the likelihood of drawing a sample from a unimodal distribution, was used to assess the statistical significance of this bimodality. In all recorded Purkinje cells ($n = 31$), the distribution of the membrane potential deviated significantly from a unimodal distribution ($P < 0.0002$, $n = 30$ cells; $P < 0.05$, $n = 1$ cell). Purkinje cells showed the characteristic electrophysiological properties reported for this cell type. As previously described[15], Purkinje cells responded to long hyperpolarizing current pulses with a slow depolarizing sag towards the prestimulus membrane potential, indicative of the presence of an I_h current (see **Supplementary Fig. 1**). The 'sag ratio', defined as the steady-state versus peak deflection during a hyperpolarizing current pulse in the down state, was 0.50 ± 0.05 (mean ± s.e.m.; $n = 11$ rat Purkinje cells). Across the population, in ketamine-xylazine–anesthetized rats, the average values of membrane potential in down and up states were –61.6 ± 0.7 mV and –44.5 ± 0.8 mV, respectively ($n = 24$ cells), generating a voltage difference between the two states of 17.1 ± 1.1 mV ($n = 24$ cells). Spontaneous fluctuations in membrane potential under barbiturate anesthesia were similar to those observed under ketamine-xylazine anesthesia, with the average membrane potential in the down state (–61.7 ± 1.4 mV, $n = 5$ cells) and the up state (–44.9 ± 1.6 mV, $n = 5$ cells) not significantly different ($P > 0.8$; **Fig. 1c**). This suggests that bimodality in Purkinje cells does not depend on the type of anesthesia used. Similar bimodality was also observed in whole-cell recordings from Purkinje cells in ketamine-xylazine–anesthetized guinea pigs ($n = 2$).

The durations of up and down states were quantified in rat Purkinje cells using long periods of continuous recording. The time spent by a Purkinje cell in a given state varied considerably between and within cells (**Fig. 1d**). The mean durations of down and up states (averaged over the mean values of each cell) were 1.50 ± 0.25 s (range: 0.41–3.61 s) and 1.45 ± 0.28 s (range: 0.25–4.84 s), respectively ($n = 17$ cells; **Fig. 1d**), and the corresponding coefficient of variance (CV) values were 0.74 ± 0.06 for down states and 0.58 ± 0.05 for up states. We also examined the time between successive transitions to the down state. The mean duration between two successive up-to-down transitions was 2.98 ± 0.48 s with a corresponding CV of 0.54 ± 0.03 ($n = 17$ cells). These results suggest that the recurrence of up and down states in Purkinje cells is rather irregular and is thus unlikely to result from a simple underlying oscillatory process (see **Supplementary Note**).

To determine whether membrane potential bimodality is an intrinsic property of Purkinje cells or whether it reflects bimodal synaptic input, we compared the intracellular activity of Purkinje cells with that of their input neurons: granule cells and molecular layer interneurons. Granule cells were identified by their depth within cerebellar cortex, their high input resistance (795 ± 88.4 MΩ, $n = 6$ cells) and their high-frequency non-accommodating spike discharge in response to strong depolarizing current pulses (**Fig. 2a**). Recordings from granule cells

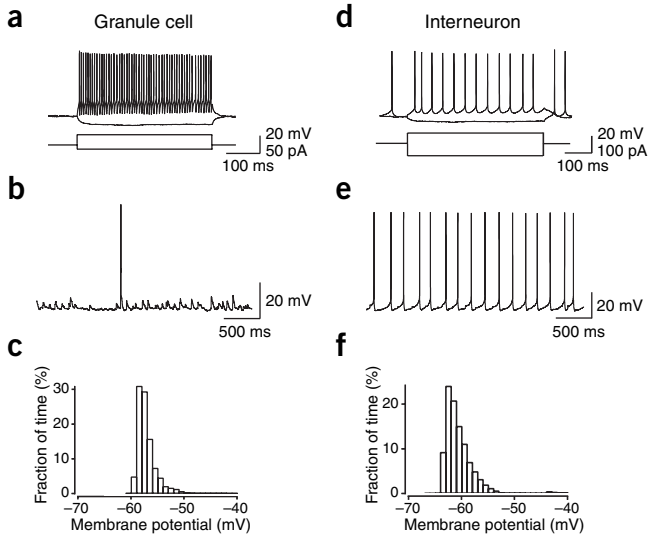

Figure 2 Membrane potential bistability is a specific feature of Purkinje cells within the cerebellar cortex. (**a**–**c**) Electrophysiological properties of rat cerebellar granule cells *in vivo*. (**a**) Voltage responses of a granule cell to hyperpolarizing (–10 pA) and depolarizing (+30 pA) current injection ($R_{in} = 872$ MΩ). (**b**,**c**) Spontaneous activity of a granule cell recorded at rest (**b**, –59 mV) and the corresponding membrane potential distribution (**c**) calculated from 20 s of recording (bin size 1 mV). (**d**–**f**) Electrophysiological properties of rat molecular layer interneurons *in vivo*. (**d**) Voltage responses of a molecular layer interneuron to hyperpolarizing (–70 pA) and depolarizing (+65 pA) current injection ($R_{in} = 103$ MΩ). (**e**,**f**) Spontaneous activity of a molecular layer interneuron recorded at rest (**e**, –63 mV) and the corresponding membrane potential distribution (**f**) calculated from 20 s of recording (bin size 1 mV). Panels **a** and **b** are from different cells, as are **d** and **e**.

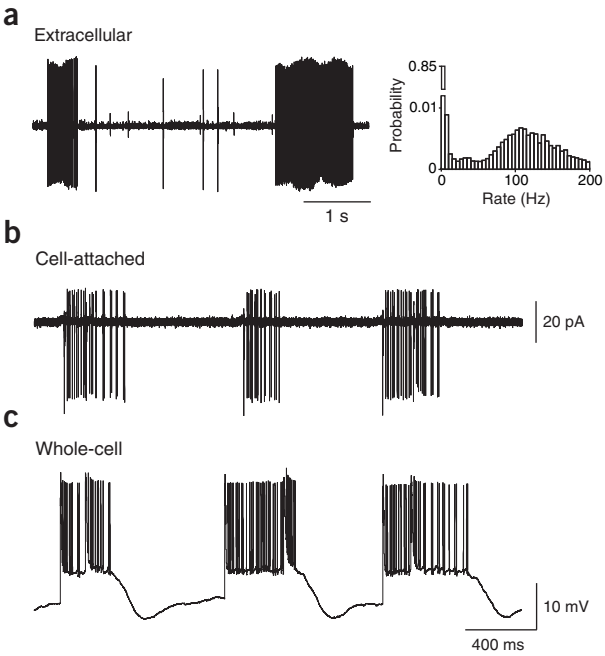

Figure 3 Membrane potential bistability is reflected in spike output pattern *in vivo*. (**a**) Left: extracellular recording from a guinea pig Purkinje cell *in vivo*. Firing pattern consisted of high-frequency bursts of simple spikes alternating with quiescent periods. Right, bimodal distribution of the instantaneous frequency of simple spikes calculated from 10 min of continuous recording (bin size 5 Hz). (**b**) Cell-attached patch-clamp recording showing the bimodal firing pattern of a rat Purkinje cell *in vivo*. (**c**) Intracellular activity of the same Purkinje cell obtained immediately after the formation of the whole-cell configuration, showing that the bimodal action potential discharge observed in the cell-attached recording reflects membrane potential bimodality.

were characterized by frequent spontaneous excitatory postsynaptic potentials that could on occasion trigger spike discharge (**Fig. 2b**). The membrane potential distribution of granule cells was unimodal ($P > 0.7$; $n = 6$ cells) with a mean membrane potential of –64.3 ± 1.9 mV (**Fig. 2c**). These properties are consistent with those previously described *in vivo* for this cell type[17]. In agreement with previous studies[18,19], molecular layer interneurons *in vivo* showed a lower input resistance (224.0 ± 34.3 MΩ, $n = 10$ cells; **Fig. 2d**) and spontaneous spiking at rest (**Fig. 2e**), which was reflected in the unimodal ($P > 0.5$, $n = 8$ cells; $P > 0.1$, $n = 2$ cells) distribution of their membrane potential around a mean value of –56.1 ± 1.4 mV (**Fig. 2f**). Granule cells and interneurons did not show bimodality even when recordings from bimodal Purkinje cells were obtained in the same preparation ($n = 5$).

The existence of two distinct states of membrane potential in Purkinje cells should be reflected in extracellular measurements of spontaneous spiking. Indeed, transitions between quiescent and spiking states were observed in our extracellular recordings *in vivo* (**Fig. 3a**). The firing pattern of guinea pig Purkinje cells recorded extracellularly consisted of high-frequency trains of simple spikes alternating with quiescent periods (**Fig. 3a**, left). This firing pattern resulted in a bimodal distribution of the instantaneous frequency of simple spikes (**Fig. 3a**, right). The prolonged periods devoid of simple spikes accounted for the peak at 0 Hz, whereas the peak around 100 Hz corresponded to the firing rate during the bursts of high-frequency simple spike firing. Across the population, the average durations of active and quiescent periods were 0.9 ± 0.2 s and 3.4 ± 0.8 s, respectively ($n = 28$ cells).

Similar spiking patterns were also observed in cell-attached recordings from rat Purkinje cells ($n = 9$ cells, **Fig. 3b**). To assess the effect of the whole-cell configuration on the membrane bimodality, we performed cell-attached and whole-cell recording in the same Purkinje cells ($n = 6$ cells; **Fig. 3b**,**c**). The intracellularly recorded membrane potential, obtained immediately after the establishment of the whole-cell configuration, showed that the bimodal simple spike discharge observed in the cell-attached recording reflected underlying membrane potential bimodality (**Fig. 3b**,**c**). The mean instantaneous frequency of simple spikes in the cell-attached configuration (102.1 ± 3.8 Hz) was comparable to that measured in the whole-cell configuration during the up state (110.7 ± 3.3 Hz; $P > 0.05$). Across the population, no significant difference in the mean firing rate between the two configurations was observed ($P > 0.6$,

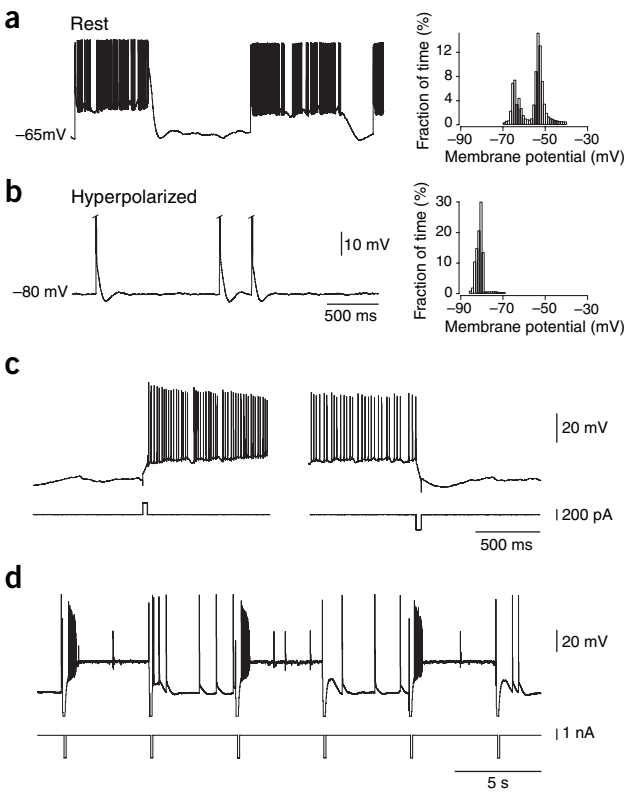

Figure 4 Intrinsic origin of membrane potential bistability *in vivo*. (**a**) Whole-cell perisomatic recording of bistable behavior of a rat Purkinje cell under barbiturate anesthesia (left). The corresponding histogram of membrane potential distribution calculated from 33 s of recording (right, bin size 1 mV) shows two distinct peaks reflecting the two states of membrane potential. (**b**) Bimodality in the same Purkinje cell was abolished by injection of negative DC current (–800 pA, left). Note the unimodal distribution of membrane potential (right, 30 s of recording, bin size 1 mV). The amplitude of spontaneous complex spikes has been truncated. (**c**) Whole-cell recordings (upper traces) of a rat Purkinje cell *in vivo* showing that the neuron can be switched from the down state to the up state and from the up state to the down state following the injection of brief depolarizing (left) and hyperpolarizing (right) current pulses, respectively (lower traces; 40 ms, 0.16 nA/–0.4 nA). (**d**) Whole-cell recording (upper trace) from a guinea pig Purkinje cell *in vivo* showing that the same hyperpolarizing current pulse (lower trace; 100 ms, 2 nA) can induce up-to-down and down-to-up transitions depending on the initial state of the membrane potential.

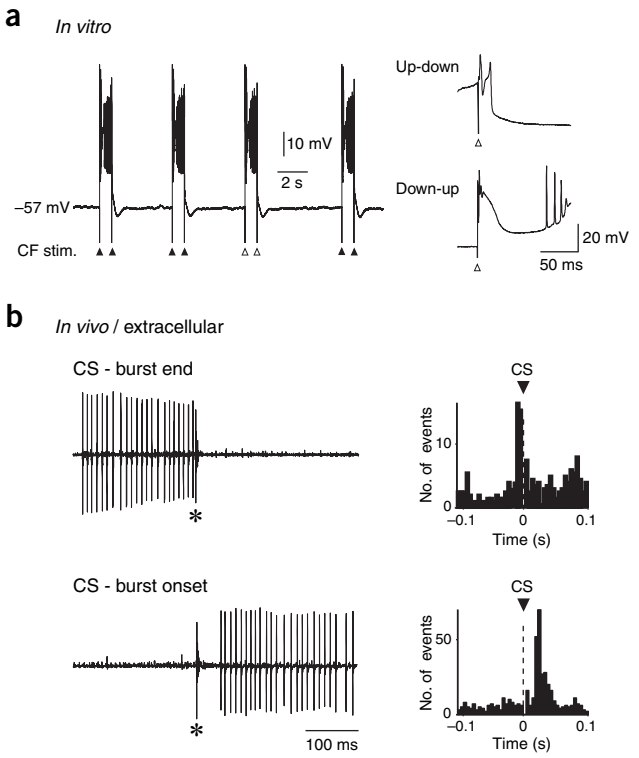

Figure 5 Climbing fiber input can trigger transitions between states. (**a**) Left: whole-cell recording from a guinea pig Purkinje cell *in vitro*. Climbing fiber stimulation (CF stim., arrowheads) triggered transitions between up states and down states in both directions. Right, expanded traces (corresponding to the open arrowheads in the left panel) showing the complex spike-evoked transitions. (**b**) Temporal relationship between complex spikes and simple spike bursts in extracellular recordings from guinea pig Purkinje cells *in vivo*. Left, representative examples of simple spike bursts followed by (top) or preceded by (bottom) a complex spike (asterisk). Right, cross-correlation of complex spikes (CS) with the end (top) and with the beginning (bottom) of bursts of simple spikes (each bin is 5 ms).

$n = 6$ cells), indicating that the whole-cell configuration did not affect the membrane potential dynamics.

To understand the origin of Purkinje cell membrane bimodality, we examined its voltage dependence. Spontaneous up and down state transitions (**Fig. 4a**) could be abolished by injection of negative DC current (–380 ± 90 pA, $n = 9$ cells), which hyperpolarized Purkinje cells to –80.6 ± 2.5 mV (**Fig. 4b**). When Purkinje cells were hyperpolarized, only complex spikes were recorded (**Fig. 4b**, left) and the membrane potential histogram (**Fig. 4b**, right) showed a bell-shaped distribution around the mean holding potential. Similarly, constant depolarizing current resulted in a single up state (data not shown). Whereas steady current injection could prevent membrane potential bimodality, brief current injections were able to induce transitions between states. Short depolarizing current pulses (0.16–1 nA, 20–100 ms duration) delivered during the down state switched the neuron to the up state with a probability of 70.5 ± 8.3% (**Fig. 4c**, left; $n = 6$ cells), whereas brief hyperpolarizing current pulses (0.2–2 nA, 20–100 ms duration) delivered during the up state could induce a transition to the down state with an efficiency of 81.5 ± 10.5% (**Fig. 4c**, right, and **Fig. 4d**; $n = 6$ cells). These reliable and almost deterministic flip-flop-like transitions are a characteristic feature of bistable systems, where transient perturbations are sufficient to induce sustained changes. Notably, hyperpolarizing current pulses delivered during the down state could also induce a transition to the up state (**Fig. 4d**). In four of five cells, hyperpolarizing current pulses (0.2–2 nA, 20–100 ms duration; $n = 5$ cells) reliably induced a down-to-up transition with a probability of 61.1 ± 14.0% (in the remaining neuron, the hyperpolarizing current pulse did not induce up states). These findings demonstrate that the bimodality of Purkinje cell membrane potential is a consequence of its bistable dynamics.

Synaptic control of intrinsic bistability

That the same current pulse can induce membrane potential transitions in both directions raised the possibility that in Purkinje cells, the same synaptic input may induce transitions between up and down states. To test this hypothesis, we first examined whether climbing fiber activation, achieved by direct electrical stimulation, could induce transitions between quiescent and spiking states in a guinea pig slice preparation. During periods of quiescence, climbing fiber activation resulted in a transition to a depolarized potential associated with simple spike discharge. Similarly, the same climbing fiber activation during an active state was capable of inducing a transition towards the lower stable state (**Fig. 5a**), thereby terminating the spontaneous discharge.

A careful examination of the records obtained *in vivo* confirmed this result. In many cases, the bursts of simple spikes recorded extracellularly were immediately followed (**Fig. 5b**, top; see Methods) or immediately preceded (**Fig. 5b**, bottom) by a complex spike (asterisk). We performed cross-correlations between complex spikes and the beginning or the end of simple spike bursts; we found a significant correlation ($P < 0.05$) between complex spikes and the end or the beginning of simple spike bursts in 75% (21 of 28) and 64% (18 of 28) of the cells, respectively (**Fig. 5b**, right).

The correlation between complex spikes and state transitions was also observed in the *in vivo* whole-cell recordings. Across the population ($n = 18$ cells), 73 ± 4% of the transitions were preceded by a complex spike, occurring less than 100 ms before the transition (**Fig. 6a**, top). A significantly lower number of transitions apparently occurred spontaneously in absence of any climbing fiber input (**Fig. 6a**, bottom; $P < 0.05$, $n = 18$ cells).

Transitions between states were characterized by a slow voltage change starting immediately after the complex spike (**Fig. 6a**, top), similar to the transitions triggered by direct climbing fiber stimulation obtained in the *in vitro* experiments (**Fig. 5a**, right). The temporal correlation between complex spikes and state transitions for one sample cell is shown (**Fig. 6b**). Up-to-down and down-to-up transitions typically occurred ~40 and ~70 ms, respectively, after a complex spike. These strong correlations allowed us to assume that state transitions occurring less than 100 ms after a complex spike were triggered by the climbing fiber activation.

Across the population ($n = 18$ cells), 62 ± 7% of the transitions to the down state and 84 ± 5% of the transitions to the up state were triggered by a climbing fiber input (**Fig. 6c**). We calculated the efficiency with which a climbing fiber input induced a transition as the ratio of the number of complex spikes that induced transitions to the total number of complex spikes. The mean frequency of complex spike firing was 0.8 ± 0.1 Hz (range: 0.2–1.7 Hz, $n = 18$ cells) and the efficiency of a complex spike in inducing a transition was 76.8 ± 4.9% ($n = 18$ cells). We also assessed the climbing fiber input efficiency in a given state. Complex spikes occurring during the up state were followed by a transition to the down state in 66.0 ± 6.4% of the cases, whereas climbing fiber input in the down state resulted in transition to the up state in 88.2 ± 3.4% of the cases ($n = 18$ cells; **Fig. 6d**). These results indicate that climbing fiber input is capable of modulating, on-line, simple spike firing pattern *in vivo*.

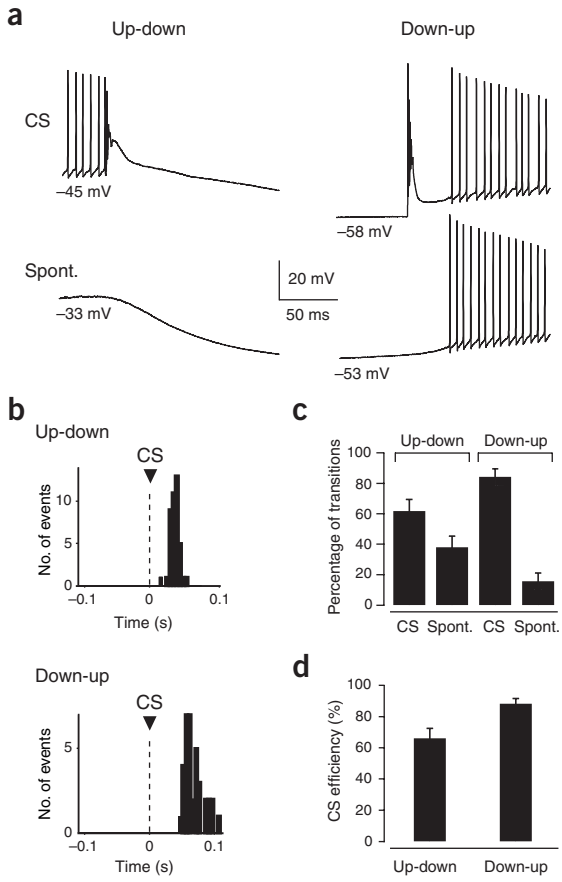

Figure 6 Characterization of the complex spike–induced transitions *in vivo*. (**a**) Whole-cell recording from a rat Purkinje cell *in vivo*, showing representative transitions between up states and down states. Most transitions (92% in this cell) are associated with complex spikes (CS, top) and only a minority occur apparently in the absence of a complex spike (Spont., bottom). (**b**) Temporal relationship between complex spikes and state transitions in a 45-min recording from a guinea pig Purkinje cell *in vivo*. Cross-correlation of complex spikes (CS) with the transition from up-to-down (top) and from down-to-up (bottom; each bin is 5 ms). (**c**) Population data from 18 rat Purkinje cell whole-cell recordings showing the percentage of up-down and down-up transitions associated with complex spikes (CS), or occurring spontaneously (Spont.). (**d**) Pooled data ($n = 18$ cells) showing the efficiency of a complex spike occurring during the up state in inducing transitions to the down state (Up-Down) and the efficiency of a complex spike occurring during the down state in inducing transitions to the up state (Down-Up).

Purkinje cell bistability modulated by sensory stimulation

The strong correlation between complex spikes and state transitions suggests that sensory stimuli that elicit complex spikes could modulate the state of the cell. To examine the influence of sensory stimulation on state transitions, we used air puff stimulation of the vibrissae or other perioral areas to activate climbing fiber inputs. In this set of experiments, recordings were performed in the Crus I and IIa of the cerebellar cortex, regions that have been shown to respond strongly to tactile stimulation of the perioral areas in anesthetized rats[20]. As illustrated by the raster plot in **Figure 7a**, air puff stimuli were effective in evoking complex spikes (filled circles). Across cells, complex spikes were evoked in 38 ± 4% of the trials ($n = 7$ cells), and comparable to previous findings[20], the latency of evoked complex spikes from the onset of the stimulus was 70 ± 7 ms (range: 47.9–93.5 ms, $n = 7$ cells). The majority of the evoked complex spikes triggered up-to-down or down-to-up transitions, depending on the initial state. In the cell shown in **Figure 7b**, 93% of the evoked complex spikes were found to be effective in triggering state transitions, with 67% inducing a transition to the down state (**Fig. 7b**, top) and 26% a transition to the up state (**Fig. 7b**, middle). In only 7% of the cases did evoked complex spikes not induce any transition (**Fig. 7b**, bottom). Across the population, 66.4 ± 11% of the evoked complex spikes were effective in triggering transitions ($n = 7$ cells). The efficiency of a complex spike evoked during the up state in inducing up-to-down transitions was 57.8 ± 15.5%, compared to 81.6 ± 7.3% for the opposite transition ($n = 7$ cells; **Fig. 7c**).

In recordings proximal enough to the soma of the Purkinje cell to allow a reliable detection of simple spikes[6], we assessed the temporal relationship between peristimulus histograms of evoked complex spikes and simple spike firing ($n = 6$; **Fig. 7d**). Evoked up-to-down and down-to-up transitions were associated with prolonged decreases (**Fig. 7d**, top) and increases (**Fig. 7d**, middle) of simple spike discharge, respectively. After the sensory-evoked up-to-down transitions, the mean simple spike firing rate was significantly reduced ($P < 0.0001$), from 57 ± 3 Hz during the baseline to 22 ± 7 Hz during the first 500 ms after the stimulus (**Fig. 7d**, top). Conversely, associated with the sensory-evoked down-to-up transitions, the mean simple spike firing rate was significantly increased ($P < 0.0001$), from 5 ± 1 Hz to 53 ± 7 Hz (**Fig. 7d**, middle). When evoked complex spikes did not trigger state transitions, we did not observe any significant change in simple spike firing compared to baseline level ($P > 0.5$; **Fig. 7d**, bottom). In the same cells, when sensory stimuli did not evoke a complex spike in the recorded Purkinje cell (**Fig. 7e**), only a slight increase (+ 7%, $P < 0.05$) in the mean simple spike firing rate was observed (**Fig. 7f**), indicating that the sensory-evoked changes in simple spike discharge resulted mainly from the state transitions triggered by the activation of climbing fiber input.

A model for bistability and state transitions

To explore the biophysical determinants of Purkinje cell membrane potential dynamics, we constructed a simplified model that emulates the fundamental features of the observed behavior: bistability, bidirectional transitions induced by outward current pulses (**Fig. 8a**, left) and bidirectional transitions induced by climbing fiber–like input (**Fig. 8a**, right). This single-compartment model consists of three ionic currents: an instantaneous, non-inactivating inward current (modeled here as a sodium current), a slow h-like current and a voltage-independent outward current (see **Supplementary Note**). The dynamic variables of this model are the membrane potential (V) and the inactivation (h) of the h-like current. Their qualitative behavior is depicted in the V-h phase plane shown in **Figure 8b**. Each point in the phase plane corresponds to a possible state of the dynamic variables of the cell model (V, h). The red and blue solid lines correspond to the $\dot{h} = 0$ and the $\dot{V} = 0$ nullclines, respectively, and the two outermost points of intersection (circles) correspond to the two stable states (stable fixed points) of the system. This bistability is primarily due to the nonlinearity of the non-inactivating inward current, which is responsible for the N-shape of the $\dot{V} = 0$ nullcline. In the hyperpolarized state (left open circle), the non-inactivating inward channels are closed and the membrane potential is determined by the combined effect of the h-like current and the voltage-independent outward current. In contrast, these channels are open in the depolarized state and will contribute substantially to the membrane potential value in the up state. The basins of attraction of the depolarized and hyperpolarized states are denoted by the blue and green areas, respectively. The separatrix, the

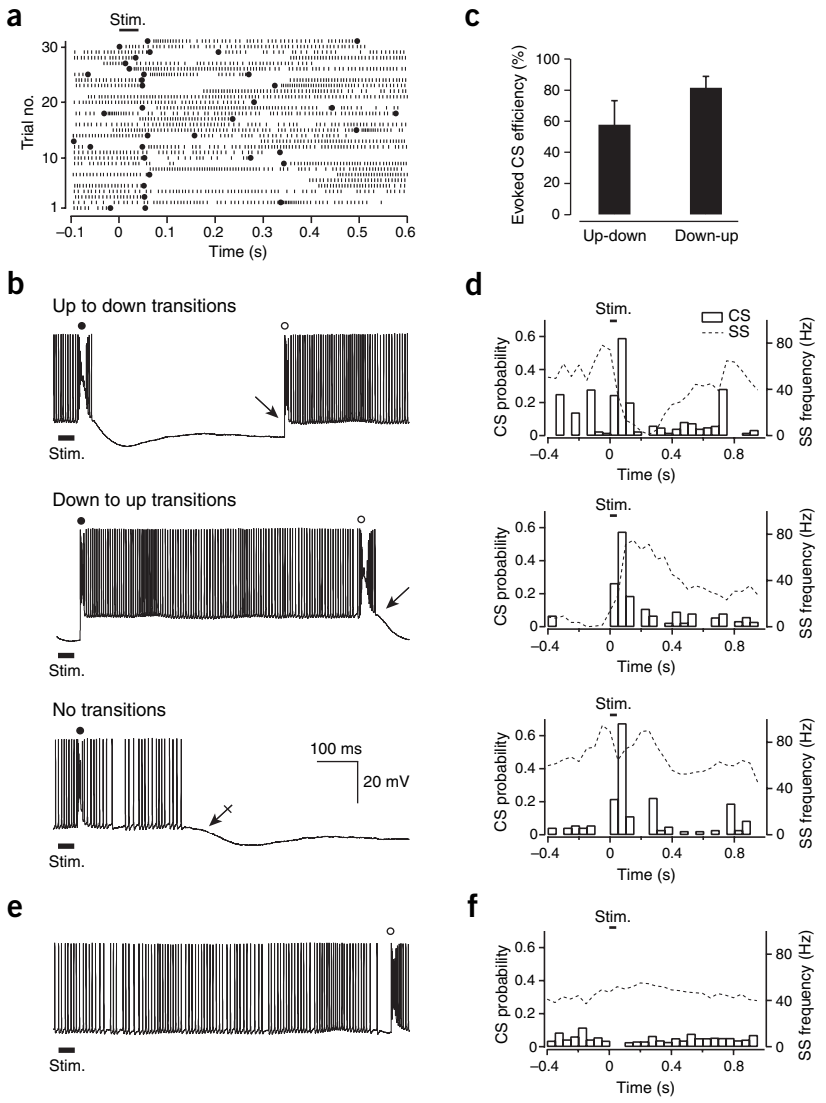

Figure 7 Sensory-evoked complex spikes in Purkinje cells can trigger membrane potential bistability *in vivo*. An air puff (40 ms) to the ipsilateral vibrissae was used to evoke responses in single Purkinje cells. (**a**) Raster plot showing the temporal relationship between sensory stimuli, complex spikes (filled circles) and simple spike firing (lines) in a rat Purkinje cell whole-cell recording *in vivo* (30 consecutive trials of 121). (**b**) Whole-cell recordings showing representative examples of sensory-evoked complex spikes (filled circles) triggering up-to-down, down-to-up, and no transitions, respectively. Note that sensory-evoked states could be interrupted by spontaneous transitions associated with spontaneous complex spikes (arrows) or occurring in the absence of complex spikes (crossed arrow). Open circles indicate spontaneously occurring complex spikes. (**c**) Pooled data ($n = 7$ cells) illustrating the efficiency of an evoked complex spike occurring during the up state in inducing transitions to the down state (Up-down) and the efficiency of an evoked complex spike occurring during the down state in inducing transitions to the up state (Down-up). (**d**) Temporal relationship between peristimulus histograms of evoked complex spikes (CS, bar chart) and simple spike firing (SS, dotted lines) on the same graph, separated into up-to-down transitions (top, $n = 5$ cells), down-to-up transitions (middle, $n = 6$ cells) and no transitions (bottom, $n = 6$ cells) (bin size 50 ms). Note that up-to-down and down-to-up transitions associated with evoked complex spikes are accompanied by robust and prolonged changes in simple spike firing. Conversely, the mean simple spike firing rate was not significantly changed compared to the baseline period (100 ms baseline, $n = 2$ cells; 500 ms baseline for the remaining cells) when evoked complex spikes did not evoke state transitions. (**e**) Example of a Purkinje cell up state in the absence of any evoked complex spikes. Open circles indicate spontaneously occurring complex spikes. (**f**) Averaged peristimulus histogram ($n = 6$ cells) of simple spike firing (dotted line) computed for sweeps where sensory stimuli did not evoke complex spikes. Trials where stimuli were delivered either during an up or a down state of the Purkinje cell were pooled together. Bar charts represent spontaneously occurring complex spikes. Results presented in **a**, **b** and **e** are from the same cell. Calibration bars in **b** apply also to **e**.

border between these areas, passes through the middle, unstable, fixed point (open square). Any voltage perturbation at either of the two fixed points that is large enough to cross the separatrix will eventually lead to the convergence of the voltage to the other fixed point. For example, a brief depolarization from the down state to a potential that is more depolarized than –54.5 mV will cross the separatrix and drive the system to the up state (trajectory not shown). Notably, climbing fiber input (modeled here as a brief, large increase in sodium conductance) delivered during the up state can have a counterintuitive effect. As a result of the depolarization, the value of the inactivation term h during the input is decreased sufficiently to allow the system to cross the separatrix into the basin of attraction of the down state (right dashed line). Thus, when the input is terminated, the dynamics converge to the down state (dash-dotted line). Conversely, a sufficiently large hyperpolarizing pulse from the down state (left dashed line) induces a substantial deinactivation of the h-like current, leading the system into the basin of attraction of the depolarized stable point. Thus, after the outward current pulse the dynamics will converge to the up state (left dash-dotted line).

Varying the properties of the outward current could affect the ability of brief hyperpolarizing current pulses or depolarizations to induce transitions between states. To study this effect, we separated the voltage-independent current into a leak and a voltage-independent potassium component. A sufficient decrease in the potassium conductance will downshift the $\dot{V} = 0$ nullcline (blue line), such that simulated climbing fiber input will induce an upward transition but not the opposite transition (**Fig. 8c**). Conversely, an increase in this conductance will upshift the $\dot{V} = 0$ nullcline such that the simulated climbing fiber input will only generate a transition to the down state (**Fig. 8d**).

To explain the spontaneous transitions between up states and down

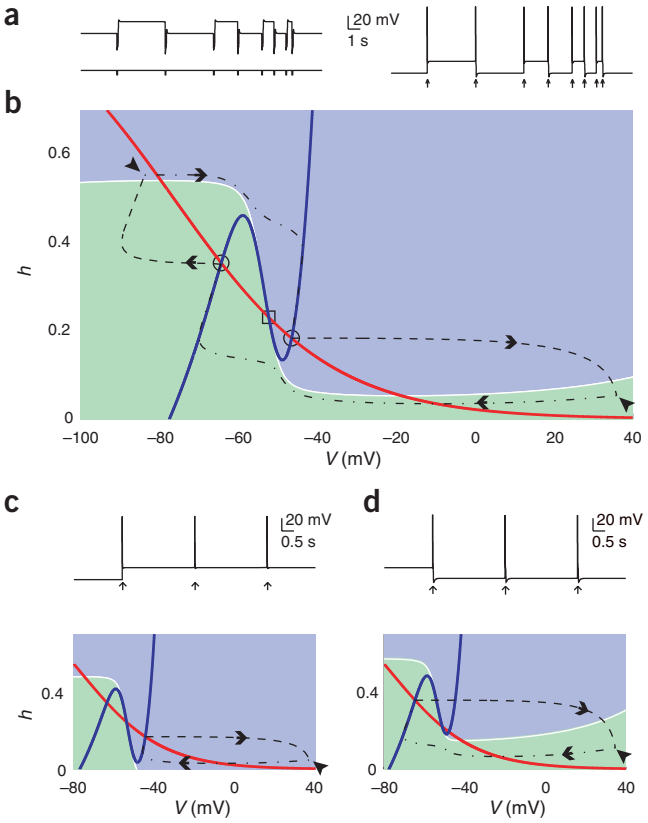

Figure 8 A model for bistability and state transitions. (**a**,**b**) Simulation of a model neuron incorporating a non-inactivating inward current, a slow h-like current, and a voltage-independent outward current. Transitions between the two stable states in both directions can be induced by brief outward current pulses (0.1 s, 7,200 nA cm^{-2}) (**a**, left) or by simulated climbing fiber input (4 ms, 1,200 μS cm^{-2} sodium conductance) (**a**, right). (**b**) Phase plane for the two dynamic variables in the model, the membrane potential V and an inactivation term h. The solid lines (red, blue) are the $\dot{h} = 0$ and the $\dot{V} = 0$ nullclines respectively; the circles denote the two stable states (fixed points) and the square denotes the unstable fixed point, which is located on the separatrix, the border between the basins of attraction of the up state (blue) and the down state (green). Arrows mark the trajectory of the dynamic variables (V, h) during (dashed lines until the diagonal arrowheads) and after (dash-dotted lines) an outward current injection (left) or a simulated climbing fiber-like input (right). (**c**) Decreasing the potassium conductance (see Results for details) shifts the $\dot{V} = 0$ nullcline down (bottom) such that the trajectory during a complex spike-like depolarization (dashed line) does not cross the separatrix. Thus, a climbing fiber input will only induce a down-to-up and not an up-to-down transition (top). (**d**) Inversely, increasing the potassium conductance shifts the nullcline up such that the trajectory during a complex spike-like depolarization (dashed line) crosses the separatrix twice (bottom). In this case, a climbing fiber input will only induce an up-to-down and not a down-to-up transition (top).

states observed *in vivo* (see **Fig. 6a**, bottom) and *in vitro*[6,15,21,22], we modified the model by replacing the voltage-independent potassium current with a slowly activating potassium current. In the absence of climbing fiber input (similar to *in vitro* conditions), this modification generated spontaneous transitions between the states, resembling those observed in slice preparations[6,15,21,22] (**Supplementary Fig. 2**). In the presence of climbing fiber–like input, this model reproduced both spontaneous and climbing fiber–evoked transitions, as well as the occasional failures of climbing fiber input to evoked a transition (see **Supplementary Note** and **Supplementary Fig. 2**).

DISCUSSION

We have demonstrated that Purkinje cells show bistability of membrane potential and spike output *in vivo*, which is a consequence of their intrinsic membrane properties. This bistability can be bidirectionally triggered by sensory-driven synaptic input, suggesting that it may represent an important intrinsic cellular mechanism for processing of sensory information in the cerebellar cortex.

Bistability of Purkinje cell output *in vivo*

Bistability of Purkinje cells *in vitro* is well-documented and has been observed to occur spontaneously[6,21,23] or after modulation of intrinsic conductances[15]. Our intracellular recordings from Purkinje cells of rats and guinea pigs anesthetized with ketamine-xylazine or pentobarbital establish that this bistability is retained *in vivo* in different animal species and under different anesthetic conditions. We further demonstrate that this bistability of membrane potential is manifested in two modes of firing activity: tonic firing of simple spikes and quiescent periods. The presence of bistability in Purkinje cell spike output is supported by previous reports showing intermittent firing patterns where periods of high-frequency, simple spike firing are interspersed with periods of quiescence in anesthetized[24] and decerebrate animals[25–27]. Similar irregular alternations between quiescence and high-frequency simple spike activity have been observed in awake recordings from various animals, including frogs[28], cats[18,29,30], squirrel monkeys[31] and rhesus monkeys[32,33]. In contrast, other cerebellar studies have not reported similar phenomena and typically find continuous firing of Purkinje cells rather than bimodal discharge, suggesting that in these cases the dynamics of Purkinje cells are not bistable. The reasons for this discrepancy are still unclear. As in other structures of the central nervous system showing intrinsic bistability, including spinal cord[8], thalamus[34] and olfactory bulb[7], this may reflect heterogeneity in the expression of bistability within a particular cell type. Furthermore, the existence of bistability in a given cell is likely to depend on neuromodulation[15,23] and on the balance of excitation and inhibition in the local network, which may depend both on the cerebellar region and the behavioral state.

Our finding that complex spikes triggered by climbing fiber input can switch Purkinje cells between up states and down states may help to resolve the discrepancy in the literature regarding the effect of complex spikes on simple spiking. Complex spikes have been shown to be associated with both increases[26,35,36] and decreases[18,24,37] in simple spike activity. Our data suggest that the effect of a complex spike on simple spike discharge depends on the state of the Purkinje cell just before the complex spike. Thus, Purkinje cells predominantly in the down state will tend to respond with an increase in simple spike activity associated with the complex spike, whereas Purkinje cells predominantly in the up state will tend to respond with a decrease. This is in agreement with the prolonged dendritic plateaus associated with increased spiking reported to be triggered by climbing fiber input in intracellular and extracellular recordings from anesthetized cats[38].

Mechanisms of bistability

Bistability is an intrinsic membrane property of Purkinje cells *in vivo*, as transitions between states can be triggered by brief hyperpolarizing and depolarizing current pulses and abolished by sufficiently strong negative or positive constant current injection. Further evidence that up states in Purkinje cells are not sustained by synaptic activity is provided by our recordings from interneurons of the molecular layer (**Fig. 2e**,**f**) and granule cells (**Fig. 2b**,**c**), the source of

parallel fiber input to both interneurons and Purkinje cells. Neither interneurons nor granule cells showed bistability, and thus it seems unlikely that up or down states are maintained by bimodal activity in the parallel fiber or interneuron input. Bistability in Purkinje cells is thus very different from the up and down states described in many cortical and striatal neurons *in vivo*. In these neurons, the up state is thought to result mainly from a continuous barrage of synaptic excitation reflecting widespread activity across the network[3,39]. In contrast, in Purkinje cells, the persistence of the two states is maintained by intrinsic voltage-dependent mechanisms. The transition between states in Purkinje cells can be triggered by the activation of the same single (albeit large) synaptic input. Notably, a recent *in vitro* study[3] has shown that the same electrical stimulus applied to the white matter of the cerebral cortex can turn on and off a network-induced up state in cortical neurons. Although the ionic and synaptic currents involved in sustaining up states and down states in these cells are different from those in Purkinje cells, our dynamical model may serve as a conceptual framework for understanding this phenomenon.

Previous simplified models for neuronal bistability in general[40] and Purkinje cell bistability in particular[41,42], as well as the present model, indicate that neither a detailed interplay between a large number of conductances nor a complex dendritic geometry are required to qualitatively generate this behavior. In our dynamical model, bistability relies on a non-inactivating inward current. However, many conductances are likely to influence the duration of states and the probability of transitions between states. Indeed, previous *in vitro* studies have shown that Purkinje cell bistability could result from interactions between non-inactivating sodium and calcium conductances with potassium conductances[6,43]. The role of the h-current (I_h) in generating the bistability is more controversial. Some *in vitro* studies have reported bistability in Purkinje cells in the presence of I_h[6,21], whereas others have shown that its downregulation, for instance by serotonin, can unmask or enhance bistability[15]. Our experiments clearly show that I_h is present in bistable Purkinje cells *in vivo* (e.g. see **Supplementary Fig. 1**; see also the depolarizing sag in **Figs. 1a**,**b**, **3c** and **4a**,**d**). This current may also have an important role in setting the voltage of the states and in controlling the transitions between the states. In particular, the ability of outward current pulses to induce bidirectional transitions requires a 'rebound' response, which is likely to result from the slow deactivation of the h-current (see **Supplementary Note**).

Purkinje cell bistability and olivo-cerebellar dynamics

The long timescale associated with Purkinje cell bistability allows a large number of different dynamical states to be sustained in the cerebellar cortex for extended periods. Each of these states is associated with a specific configuration of up and down states in different Purkinje cells. These network states can be used to maintain specific functional networks within the olivary nucleus: the sustained firing state of a Purkinje cell inhibits neurons in the deep cerebellar nuclei, which in turn remove the inhibition from the electrically coupled dendrites of the inferior olive neurons, producing synchronized rhythmic activity in a subset of olivary neurons. Notably, recordings of deep cerebellar nucleus neurons show prolonged (up to 0.5 s) inhibitory responses to brief sensory stimulation (N.C. Rowland and D. Jaeger, *Soc. Neurosci. Abstr.* 75.10, 2003), which may correspond to synchronized up states in presynaptic Purkinje cells activated by sensory stimulation.

Computational implications of bistability

The presence of bistability may have important implications for integration of mossy fiber input to the cerebellar cortex mediated by the parallel fiber pathway. First, the responsiveness of the Purkinje cell to sensory-evoked parallel fiber input will depend on whether previous climbing fiber input has switched the Purkinje cell into the up state or down state. This suggestion is consistent with previous work showing that the gain of Purkinje cell responses to sensory-driven mossy fiber input depends on the recent history of climbing fiber activity on the time scale of hundreds of milliseconds[44]. Second, given that bistability is also observed in the distal dendrites, the activation of voltage-gated dendritic conductances[6] will also be influenced. In particular, activation of dendritic calcium spikes by parallel fiber input is strongly voltage and time dependent[45]. Given that calcium spikes have been implicated in the induction of long-term depression (LTD) at parallel fiber synapses[46], the fact that sensory-evoked climbing fiber inputs can induce prolonged depolarizations provides a possible cellular substrate for climbing fiber–dependent forms of parallel fiber plasticity in which a broad time window for induction (several hundred milliseconds) has been observed[38]. Purkinje cell bistability may therefore contribute to determining the rules for LTD induction in the intact cerebellar network.

Chemical synapses have traditionally been classified as either excitatory or inhibitory according to their effect on the firing rate of the postsynaptic neuron. In this study we have demonstrated that the same synapse can play both roles. The activation of climbing fiber synapses can either increase or decrease the firing rate of the Purkinje cell, depending on its initial state. This property, in which the same input induces both transitions in a bistable element, is known in electronics as a 'toggle switch', which is widely used in electrical devices. We suggest that toggling of the Purkinje cells may serve as a higher-order reflex that generates an immediate and reflexive response of the system to the occurrence of an error by shifting the Purkinje cell activity away from its current erroneous operating state.

METHODS

The care and experimental manipulation of the animals was carried out in accordance with the regulations of the Hebrew University of Jerusalem and the U.K. Home Office.

***In vivo* recordings.** Sprague-Dawley rats (P18–P27) or Dunkin-Hartley guinea pigs (180–300 g) were anesthetized by intraperitoneal injection of ketamine (50 mg kg^{-1})-xylazine (3 mg kg^{-1}) or pentobarbital (60 mg kg^{-1}). The level of anesthesia was routinely monitored by observing whisker movements or the response to a noxious stimulus to the hind limbs, and additional doses of anesthetic were added as needed. The animals were placed in a stereotaxic apparatus, and the occipital bone and the dura mater were removed, exposing a small region of the cerebellar vermis or hemispheres. The exposed area was covered with physiological saline or agar (3% in physiological or saline solutions). Sensory responses were evoked by an air puff (30–70 ms, 40 psi) timed by a custom pressure device and delivered to the ipsilateral perioral surface.

Cell-attached and whole-cell patch-clamp recordings were made with a Multiclamp 700A or an Axoclamp 2B amplifier (Axon Instruments) using previously described techniques[47]. The pipette solution contained 130 mM potassium methanesulfonate, 7 mM KCl, 10 mM HEPES, 0.05 mM EGTA, 2 mM MgATP, 2 mM Na_2ATP and 0.5 mM Na_2GTP, pH 7.2, in recordings from rats, or 140 mM potassium gluconate, 4 mM NaCl, 10 mM HEPES, 4 mM MgATP, 1 mM EGTA and 0.1 mM $CaCl_2$, pH 7.4, for guinea pig recordings. Extracellular recordings of guinea pig Purkinje cell single-unit activity were obtained using glass pipette electrodes, pulled to a DC resistance of 10–20 MΩ and filled with 2 M NaCl. A differential AC amplifier (DP-301; Warner Instruments) was used for monitoring ongoing activity. Recordings were filtered at 3–10 kHz and sampled at 20–50 kHz using an Instrutech (ITC-18) or National Instruments (PCI-MIO-16XE-10) analog to digital board.

Slice recordings. The *in vitro* experiments were performed on 300 μm thick sagittal slices of cerebellar vermis from guinea pigs (180–200g). Preparation of slices and recording techniques are described elsewhere[48]. Recordings were

performed at 27–30 °C or at room temperature (22–25 °C) in physiological solution containing 124 mM NaCl, 5 mM KCl, 1.3 mM $MgSO_4$, 1.2 mM KH_2PO_4, 26 mM $NaHCO_3$, 10 mM glucose, and 2.4 mM $CaCl_2$.

Analysis. Correlation between complex spikes and state transitions in intracellular recordings was performed in Purkinje cells where the identification of complex spikes was unambiguous. The response of the membrane potential to climbing fiber input during the up and down states could differ considerably (see **Figs. 5a** and **6a**). During the down state, complex spikes were characterized by a large-amplitude spike followed by a burst of smaller spikes and a long depolarization[6]. During the up state, complex spikes were characterized by a stereotypic waveform, composed of several fast distinct peaks. The rate of these complex spikes was independent of the state of the cell. Simple and complex spikes recorded extracellularly were sorted offline according to their amplitude and shape, using an adaptive template routine in MATLAB (version 6.0, Mathworks). To control the quality of sorting, all simple spikes and complex spikes were superimposed and examined visually. Cells were discarded from the analysis if the estimated number of errors in sorting exceeded 2%.

Histograms of membrane potential distribution were constructed for each Purkinje cell, and Gaussian fits were applied to the individual peaks. The modal value of each Gaussian fit was taken as the mean membrane potential for the up state and the down state. To measure the duration of each individual sate, transitions between the up and down states were detected using the following thresholding procedure: two thresholds were set at one-fourth and three-fourths of the distance between the peaks of the membrane potential distribution. When the membrane potential rose above the lower threshold, a down-to-up transition was registered; when the membrane potential fell below the upper threshold, an up-to-down transition was registered. To avoid defining noise or individual complex spikes as a short state, we removed pairs of lower and upper thresholds generating a time difference of less than 100 ms. Up and down state durations were quantified in Purkinje cells where the duration of the recordings was long enough to allow measurement of at least 15 up and down states. The deviation from unimodality of the membrane potential of Purkinje cells, as well as that of granule cells and molecular interneurons, was tested using a 'dip test'[16], using software R (version 1.9.1; http://www.R-project.org). For each cell, the test was performed using 500 randomly chosen values of membrane potential.

In extracellular and cell-attached recordings, we defined a burst of simple spikes as an event that is flanked by periods of at least 100 ms devoid of simple spikes (qualitatively similar results were obtained using other criteria). Correlations between complex spikes and the beginning of a burst were calculated using a window of 50 ms, starting 25 ms after the complex spike. Correlations between complex spikes and the end of a burst were calculated using a window of 40 ms preceding the complex spike. The use of different windows did not produce a qualitative difference in the results.

Input resistance (R_{in}) was calculated from steady-state voltage deflections during (400–500 ms) step hyperpolarizing current injections (granule cells, 5–10 pA; molecular layer interneurons, 20–70 pA). Additional data analysis was carried out using Igor Pro (Wavemetrics). Data are mean ± s.e.m. unless otherwise indicated. Statistical comparisons were made using Student's paired or unpaired *t*-test.

Note: Supplementary information is available on the Nature Neuroscience website.

ACKNOWLEDGMENTS

We thank H. Meiri, E. Chorev and P. Mann-Metzer for excellent technical assistance, J.T. Davie for help with programming, and J.I. Simpson and T. Margrie for encouragement and helpful discussions. This work was supported by grants from the European Commission (M.H. and Y.Y.), Wellcome Trust (M.H and S.M), Gatsby Foundation (M.H), JSPS (K.K.), US-Israel BSF (Y.Y.), the Israel Science Foundation (Y.Y.), the Israel Science Foundation Center of Excellence 8006-00 (H.S.) and the Yeshaya Horowitz Association (Y.L.).

COMPETING INTERESTS STATEMENT

The authors declare that they have no competing financial interests.

Received 20 October 2004; accepted 3 January 2005
Published online at http://www.nature.com/natureneuroscience/

1. Fuster, J.M. Unit activity in prefrontal cortex during delayed-response performance: neuronal correlates of transient memory. *J. Neurophysiol.* **36**, 61–78 (1973).
2. McCormick, D.A. *et al.* Persistent cortical activity: mechanisms of generation and effects on neuronal excitability. *Cereb. Cortex* **13**, 1219–1231 (2003).
3. Shu, Y., Hasenstaub, A. & McCormick, D.A. Turning on and off recurrent balanced cortical activity. *Nature* **423**, 288–293 (2003).
4. Camperi, M. & Wang, X.J. A model of visuospatial working memory in prefrontal cortex: recurrent network and cellular bistability. *J. Comput. Neurosci.* **5**, 383–405 (1998).
5. Marder, E., Abbott, L.F., Turrigiano, G.G., Liu, Z. & Golowasch, J. Memory from the dynamics of intrinsic membrane currents. *Proc. Natl. Acad. Sci. USA* **93**, 13481–13486 (1996).
6. Llinas, R. & Sugimori, M. Electrophysiological properties of *in vitro* Purkinje cell somata in mammalian cerebellar slices. *J. Physiol. (Lond.)* **305**, 171–195 (1980).
7. Heyward, P., Ennis, M., Keller, A. & Shipley, M.T. Membrane bistability in olfactory bulb mitral cells. *J. Neurosci.* **21**, 5311–5320 (2001).
8. Lee, R.H. & Heckman, C.J. Bistability in spinal motoneurons *in vivo*: systematic variations in persistent inward currents. *J. Neurophysiol.* **80**, 583–593 (1998).
9. Egorov, A.V., Hamam, B.N., Fransen, E., Hasselmo, M.E. & Alonso, A.A. Graded persistent activity in entorhinal cortex neurons. *Nature* **420**, 173–178 (2002).
10. Koulakov, A.A., Raghavachari, S., Kepecs, A. & Lisman, J.E. Model for a robust neural integrator. *Nat. Neurosci.* **5**, 775–782 (2002).
11. Goldman, M.S., Levine, J.H., Major, G., Tank, D.W. & Seung, H.S. Robust persistent neural activity in a model integrator with multiple hysteretic dendrites per neuron. *Cereb. Cortex* **13**, 1185–1195 (2003).
12. Loewenstein, Y. & Sompolinsky, H. Temporal integration by calcium dynamics in a model neuron. *Nat. Neurosci.* **6**, 961–967 (2003).
13. Häusser, M. & Clark, B.A. Tonic synaptic inhibition modulates neuronal output pattern and spatiotemporal synaptic integration. *Neuron* **19**, 665–678 (1997).
14. Ito, M. *The Cerebellum and Neural Control* (Raven, New York, 1984).
15. Williams, S.R., Christensen, S.R. Stuart, G J. & Häusser, M. Membrane potential bistability is controlled by the hyperpolarization- activated current I(H) in rat cerebellar Purkinje neurons in vitro. *J. Physiol. (Lond.)* **539**, 469–483 (2002).
16. Hartigan, J.A. & Hartigan, P.M. The dip test of unimodality. *Ann. Stat.* **13**, 70–84 (1985).
17. Chadderton, P., Margrie, T.W. & Häusser, M. Integration of quanta in cerebellar granule cells during sensory processing. *Nature* **428**, 856–860 (2004).
18. Armstrong, D.M. & Rawson, J.A. Activity patterns of cerebellar cortical neurones and climbing fibre afferents in the awake cat. *J. Physiol. (Lond.)* **289**, 425–448 (1979).
19. Jorntell, H. & Ekerot, C.F. Receptive field plasticity profoundly alters the cutaneous parallel fiber synaptic input to cerebellar interneurons *in vivo*. *J. Neurosci.* **23**, 9620–9631 (2003).
20. Brown, I.E. & Bower, J.M. Congruence of mossy fiber and climbing fiber tactile projections in the lateral hemispheres of the rat cerebellum. *J. Comp. Neurol.* **429**, 59–70 (2001).
21. Rapp, M., Segev, I. & Yarom, Y. Physiology, morphology and detailed passive models of guinea-pig cerebellar Purkinje cells. *J. Physiol. (Lond.)* **474**, 101–118 (1994).
22. Chang, W., Strahlendorf, J.C. & Strahlendorf, H.K. Ionic contributions to the oscillatory firing activity of rat Purkinje cells in vitro. *Brain Res.* **614**, 335–341 (1993).
23. Hounsgaard, J. & Midtgaard, J. Intrinsic determinants of firing pattern in Purkinje cells of the turtle cerebellum *in vitro*. *J. Physiol. (Lond.)* **402**, 731–749 (1988).
24. Bell, C.C. & Grimm, R.J. Discharge properties of Purkinje cells recorded on single and double microelectrodes. *J. Neurophysiol.* **32**, 1044–1055 (1969).
25. Brookhart, J.M., Moruzzi, G. & Snider, R.S. Spike discharges of single units in the cerebellar cortex. *J. Neurophysiol.* **13**, 465–486 (1950).
26. McDevitt, C.J., Ebner, T.J. & Bloedel, J.R. The changes in Purkinje cell simple spike activity following spontaneous climbing fiber inputs. *Brain Res.* **237**, 484–491 (1982).
27. Granit, R. & Phillips, C.G. Excitatory and inhibitory processes acting upon individual Purkinje cells of the cerebellum in cats. *J. Physiol. (Lond.)* **133**, 520–547 (1956).
28. Nacimiento, R.C. Spontaneous and evoked discharges of cerebellar Purkinje cells in the frog. in *Neurobiology of Cerebellar Evolution and Development* (ed. Llinas, R.) 373–395 (American Medical Assn., Chicago, 1969).
29. McCarley, R.W. & Hobson, J.A. Simple spike firing patterns of cat cerebellar Purkinje cells in sleep and waking. *Electroencephalogr. Clin. Neurophysiol.* **33**, 471–483 (1972).
30. Edgley, S.A. & Lidierth, M. Step-related discharges of Purkinje cells in the paravermal cortex of the cerebellar anterior lobe in the cat. *J. Physiol. (Lond.)* **401**, 399–415 (1988).
31. Hirata, Y. & Highstein, S.M. Analysis of the discharge pattern of floccular Purkinje cells in relation to vertical head and eye movement in the squirrel monkey. *Prog. Brain Res.* **124**, 221–232 (2000).
32. Bauswein, E., Kolb, F.P. & Rubia, F.J. Cerebellar feedback signals of a passive hand movement in the awake monkey. *Pflugers Arch.* **402**, 292–299 (1984).
33. Kobayashi, Y. *et al.* Temporal firing patterns of Purkinje cells in the cerebellar ventral paraflocculus during ocular following responses in monkeys II. Complex spikes. *J. Neurophysiol.* **80**, 832–848 (1998).
34. Williams, S.R., Toth, T.I., Turner, J.P., Hughes, S.W. & Crunelli, V. The 'window' component of the low threshold Ca2+ current produces input signal amplification and bistability in cat and rat thalamocortical neurones. *J. Physiol. (Lond.)* **505**, 689–705 (1997).
35. Rawson, J.A. & Tilokskulchai, K. Repetitive firing of cerebellar Purkinje cells in response to impulse in climbing fibre afferents. *Neurosci. Lett.* **25**, 131–135 (1981).
36. Sato, Y., Miura, A., Fushiki, H. & Kawasaki, T. Short-term modulation of cerebellar Purkinje cell activity after spontaneous climbing fiber input. *J. Neurophysiol.* **68**, 2051–2062 (1992).

37. Rawson, J.A. & Tilokskulchai, K. Suppression of simple spike discharges of cerebellar Purkinje cells by impulses in climbing fibre afferents. *Neurosci. Lett.* **25**, 125–130 (1981).
38. Ekerot, C.F. & Kano, M. Long-term depression of parallel fibre synapses following stimulation of climbing fibres. *Brain Res.* **342**, 357–360 (1985).
39. Mahon, S., Deniau, J.M. & Charpier, S. Relationship between EEG potentials and intracellular activity of striatal and cortico-striatal neurons: an *in vivo* study under different anesthetics. *Cereb. Cortex* **11**, 360–373 (2001).
40. Rinzel, J. & Ermentrout, B. Analysis of Neural Excitability and Oscillations in *Methods of Neuronal Modeling* (eds. Koch, C. & Segev, I.) 251–291 (MIT Press, Cambridge, 1998).
41. Yuen, G.L., Hockberger, P.E. & Houk, J.C. Bistability in cerebellar Purkinje cell dendrites modelled with high- threshold calcium and delayed-rectifier potassium channels. *Biol. Cybern.* **73**, 375–388 (1995).
42. Genet, S. & Delord, B. A biophysical model of nonlinear dynamics underlying plateau potentials and calcium spikes in Purkinje cell dendrites. *J. Neurophysiol.* **88**, 2430–2444 (2002).
43. Llinas, R. & Sugimori, M. Electrophysiological properties of in vitro Purkinje cell dendrites in mammalian cerebellar slices. *J. Physiol. (Lond.)* **305**, 197–213 (1980).
44. Ebner, T.J. & Bloedel, J.R. Role of climbing fiber afferent input in determining responsiveness of Purkinje cells to mossy fiber inputs. *J. Neurophysiol.* **45**, 962–971 (1981).
45. Midtgaard, J., Lasser-Ross, N. & Ross, W. Spatial distribution of Ca^{2+} influx in turtle Purkinje cell dendrites in vitro: role of a transient outward current. *J. Neurophysiol.* **70**, 2455–2469 (1993).
46. Wang, S.S., Denk, W. & Häusser, M. Coincidence detection in single dendritic spines mediated by calcium release. *Nat. Neurosci.* **3**, 1266–1273 (2000).
47. Margrie, T.W., Brecht, M. & Sakmann, B. *In vivo*, low-resistance, whole-cell recordings from neurons in the anaesthetized and awake mammalian brain. *Pflugers Arch.* **444**, 491–498 (2002).
48. Mann-Metzer, P. & Yarom, Y. Electrotonic coupling interacts with intrinsic properties to generate synchronized activity in cerebellar networks of inhibitory interneurons. *J. Neurosci.* **19**, 3298–3306 (1999).